Turkish Journal of Engineering & Environmental Sciences

http://journals.tubitak.gov.tr/engineering/

Research Article

Turkish J Eng Env Sci
(2013) 37: 231 – 246

doi:10.3906/muh-1212-13

Electro-thermo–mechanical nonlinear buckling of Pasternak coupled DWBNNTs based on nonlocal piezoelasticity theory

Ali GHORBANPOUR ARANI[1,2,*], Seyed Abolfazl JAMALI[1], Saeed AMIR[1], Mohammad Javad MABOUDI[1]

[1]Faculty of Mechanical Engineering, University of Kashan, Kashan, Iran
[2]Institute of Nanoscience & Nanotechnology, University of Kashan, Kashan, Iran

Received: 24.12.2012 • **Accepted:** 11.09.2013 • **Published Online:** 03.02.2014 • **Printed:** 28.02.2014

Abstract: Nonlinear buckling of bonded double-walled boron nitride nanotubes (DWBNNTs) under combined electro-thermo–mechanical loadings based on the nonlocal piezoelasticity theory and Euler–Bernoulli beam (EBB) model is presented in this paper. Coupled DWBNNTs are embedded in an elastic medium that is simulated as a Pasternak foundation. Using the Lennard-Jones model, the van der Waals interaction between 2 layers of DWBNNTs is taken into account. Considering the von Kármán geometric nonlinearity, Hamilton's principle, and charge equation, higher order governing equations are derived and solved by differential quadrature method (DQM). The detailed parametric study is conducted, focusing on the remarkable effects on the behavior of nonlinear buckling loads. The results indicated that the small-scale parameter, elastic medium, boundary conditions, electric potential, aspect ratio, and different vibration phases play an important role in the nonlinear buckling of smart elastically coupled systems. In addition, it is found that the trend of figures has good agreement with those of previous research. The results of this work could be used in the design and manufacture of nano/micro-electro–mechanical systems.

Key words: Nonlinear buckling, coupled system, nonlocal piezoelasticity theory, energy method, DQM

1. Introduction

Theoretical and experimental studies of nanostructures such as nanowires and nanotubes have received much attention since the identification of carbon nanotubes (CNTs) [1]. Many investigations have focused on modern nanotechnology involving nanotubes embedded in an elastic matrix because of their great importance in the development of nanodevices.

Rubio et al. [2] proposed the existence of boron nitride nanotubes (BNNTs) for the first time. BNNTs are similar in structure to CNTs in which C atoms are substituted by alternating B and N atoms. They have become the most promising materials for nanoelectronics, nanodevices, and nanocomposites because of their novel properties [3]. They are different as far as high temperature resistance to oxidation (>900 °C) and possessing strong piezoelectric characteristics are concerned [4]. The electrical properties of CNTs are strongly affected by the rolling angle of the nanotube lattice molecular structure, known as chirality, which has limited the applications of CNTs in electrical components, especially in nanoelectrical devices [5]. BNNTs possess extraordinary properties such as high elastic modulus, high thermal conductivity, low density, constant wide band gap, superb structural stability, and chemical inertness [6]. Meanwhile, they have more resistance to

*Correspondence: aghorban@kashanu.ac.ir

oxidation at high temperature than other conventional nanotubes such as CNTs and they are used for high temperature applications [7]. Mechanical and electrical properties of BNNTs have been of interest to researchers due to their piezoelectric properties.

In recent years, a large number of studies have been carried out on buckling and vibration of nanotubes/microtubes. Based on the nonlocal elasticity theory on mechanical behavior, Eringen [8] indicated that the stress at a point is related to the strain at all points of the body. Wang and Varadan [9] studied vibration of both single-walled nanotubes and double-walled nanotubes via nonlocal elastic beam theories where they considered small-scale effects on vibration characteristics of CNTs. Wang et al. [10] investigated the elastic buckling analysis of micro- and nanorods/tubes based on Eringen's nonlocal elasticity theory and the Timoshenko beam theory. Explicit expressions for the critical buckling loads were derived for axially loaded rods/tubes with various end conditions. They showed that the sensitivity of the small-scale effect on the buckling loads may be observed. Various available beam theories, including the Euler–Bernoulli, Timoshenko, Reddy, and Levinson beam theories were reformulated using the nonlocal differential constitutive relations of Eringen by Reddy [11]. Analytical solutions of bending, vibration and buckling were presented using the nonlocal theories to bring out the effect of the nonlocal behavior on deflections, buckling loads, and natural frequencies. Aydogdu [12] proposed a generalized nonlocal beam theory to study bending, buckling, and free vibration of nanobeams. Ghorbanpour Arani et al. [13] investigated the free transverse vibrations of single-walled carbon nanotubes (SWCNTs) and double-walled carbon nanotubes (DWCNTs) under axial load using EBB, Timoshenko beam, and Donnell shell models. Their results showed that the natural frequencies predicted by nonlocal theory are lower than those of classical theory. In another study, Ghorbanpour Arani et al. [14] presented the thermal effect on the buckling of DWCNTs resting on the Pasternak foundation using Eringen's partial nonlocal elasticity theory. They concluded that the strength of a DWCNT was related to the Winkler and shear modules. Akgöz and Civalek [15] discussed the effects of length parameter on the buckling characteristics of micro-sized beams with hinged–hinged and clamped–free boundary conditions.

Buckling of BNNTs in a PVDF matrix as an elastic medium subjected to combined electro-thermo–mechanical loadings was investigated by Salehi-Khojin and Jalili [16], who showed that applying direct and reverse voltages to BNNT changed buckling loads for any axial and circumferential wave numbers. Later, axial buckling analysis of embedded DWBNNTs under combined electro-thermo–mechanical loadings was presented by Ghorbanpour Arani et al. [17]. They concluded that the electric field and its direction have significant effects on the magnitude of the critical buckling load.

On the other hand, Murmu and Adhikari [18] analyzed nonlocal vibration of bonded double-nanoplate systems. Their study highlighted that the small-scale effects considerably influence the transverse vibration of a double-nanoplate system. Moreover, they elucidated that increasing stiffness of the coupling springs in a nonlocal coupled system causes a decrease in the small-scale effects during the asynchronous modes of vibration. Furthermore, nonlocal buckling behavior of coupled nanoplate systems was reported by Murmu et al. [19], who showed that the effect of nonlocal parameter values for the case of synchronous buckling modes is higher than for the asynchronous state. Vibration analysis of the coupled system of double-layered graphene sheets embedded in a Visco-Pasternak foundation was carried out by Ghorbanpour Arani et al. [20] based on nonlocal elasticity theory. Their results indicated that the effect of nonlocal parameter decreases for higher values of the Winkler and Pasternak modulus.

However, to date, no report has been found in the literature on the buckling behavior of coupled DWBNNT systems embedded in an elastic medium. Motivated by this consideration, this study aims to present

the investigation of nonlinear buckling analysis of coupled DWBNNT systems under combined electro-thermo–mechanical loadings. Coupled DWBNNTs are embedded with an elastic medium simulated by Pasternak type as spring and shear foundations. Using nonlocal piezoelasticity theory the nonlinear buckling response of coupled DWBNNTs is obtained. In order to obtain the critical buckling load of the coupled system, using Hamilton's principle, the higher-order governing equations of motion are derived and solved by DQM. The effects of nonlocal parameter, aspect ratio, elastic medium coefficients, and different boundary conditions on the buckling behavior of the coupled system for different states are taken into account. In order to validate this study, the results obtained by Murmu and Pradhan [21] and Wang et al. [10] are compared with the results of the present work.

2. Nonlocal Piezoelectricity theory

In the classical theory of continuum mechanics, the stress at a point is only dependent on strain at that point, while according to Eringen nonlocal elasticity theory [8] the stress at a point is related to the strain at all points of the body. This phenomenon is known as small-scale effect, and is shown in constitutive equations by the parameter e_0a. Recently, the nonlocal elasticity theory has been applied for nano/microstructures in the literature by Ghorbanpour Arani et al. [22]. The nonlocal constitutive equations for a homogeneous and piezoelectric nanostructure are written as:

$$(1-(e_0a)^2\nabla^2)\,\sigma=\tau \tag{1a}$$

$$(1-(e_0a)^2\nabla^2)\,D=\Gamma, \tag{1b}$$

where σ and τ are nonlocal and local stresses, respectively, and D and Γ are nonlocal and local electric displacements, respectively. e_0a and ∇^2 are the small-scale parameter and Laplace operator, respectively, where e_0 denotes an appropriate constant for each material and a is an internal characteristic length of the material (e.g., length of B-N bond, lattice spacing, granular distance), where $a=0.145\,nm$ for BNNTs [23]. The local stress relation for piezoelectric materials under electro-thermal loading is [24]:

$$\{\tau\}=[c]\{\varepsilon\}-[h]^T\{E\}-\{\lambda\}T, \tag{2}$$

where $\{h\}$, $\{E\}$, and $\{\lambda\}$ are strain vector, electric field, and thermal expansion, respectively; $[C]$, $[h]$, and T denote matrices of elastic stiffness, piezoelectric parameter, and temperature change, respectively. Zigzag structures for BNNTs have been considered in this study due to the favorable axial piezoelectric response to tension and compression. For the EBB model, the stress-strain relation for piezoelectric materials under electro-thermal axial loading is:

$$\tau_{xx}=C_{11}\varepsilon_x-h_{11}E_x-C_{11}\alpha_xT \tag{3}$$

and local electric displacement relation based on piezoelasticity theory is:

$$\Gamma_x=h_{11}(\varepsilon_x-\alpha_xT)+\in_{11}E_x, \tag{4}$$

where $\in_{11}$ denotes the dielectric constant for isotropic material and E_x is defined as [24]:

$$E_x=-\frac{\partial\varphi}{\partial x}, \tag{5}$$

where φ is the electric potential.

3. Governing relations

Figure 1 illustrates 2 DWBNNTs coupled by Pasternak medium where the inner and outer radii of the DWBNNTs are $r_{12} = r_{22}$ and $r_{11} = r_{21}$, respectively; L and h are length and thickness, respectively. Based on EBB theory the general displacement fields are [24]:

$$\begin{aligned} \tilde{U}(x,z,t) &= U(x,t) - z\frac{\partial W(x,t)}{\partial x} \\ \tilde{V}(x,z,t) &= 0 \\ \tilde{W}(x,z,t) &= W(x,t) \end{aligned} \tag{6}$$

U Band W are the components of the middle surface displacement (i.e. displacement at $z = 0$), and nonlinear strain–displacement relations can be demonstrated as:

$$\begin{aligned} \varepsilon_{xx}(x,z) &= \frac{\partial \tilde{U}}{\partial x} + \frac{1}{2}(\frac{\partial \tilde{W}}{\partial x})^2 = \frac{\partial U}{\partial x} - z\frac{\partial W}{\partial x} + \frac{1}{2}(\frac{\partial W}{\partial x})^2 \\ \varepsilon_{zz}(x,z) &= 0 \\ \gamma_{xz}(x,z) &= 0 \end{aligned} \tag{7}$$

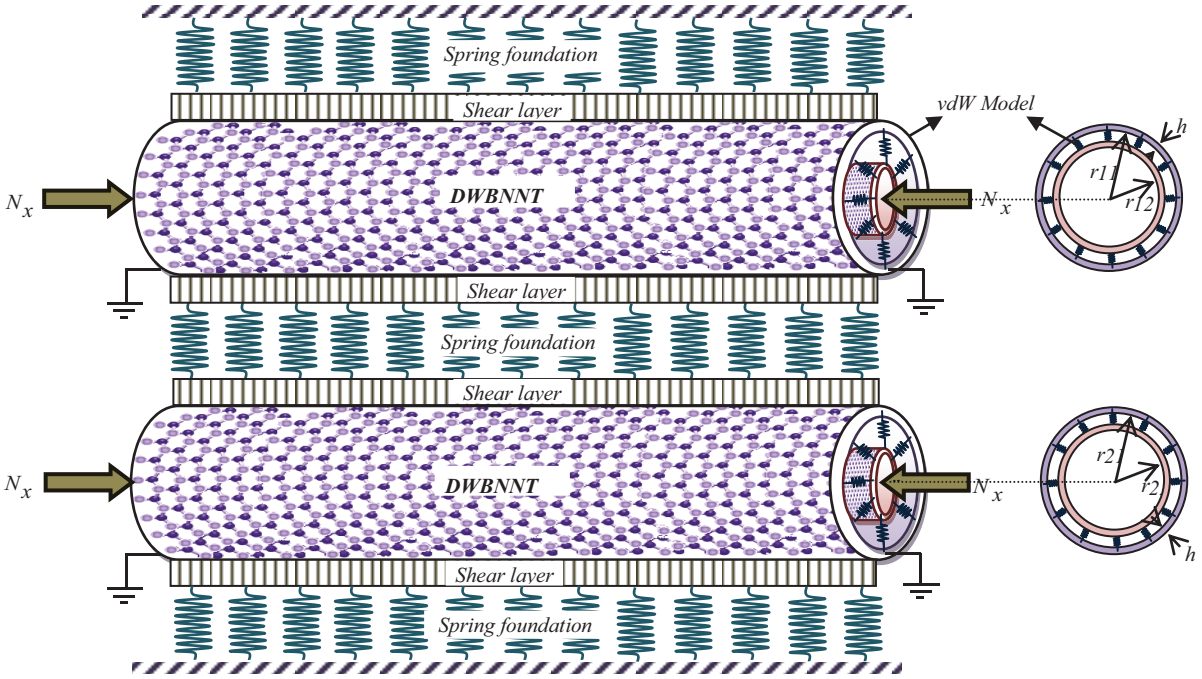

Figure 1. Schematic of 2 DWBNNTs coupled by a Pasternak foundation.

3.1. Electrostatic potential energy

Electrostatic potential energy ($\prod$) for each layer of DWBNNT is [24]:

$$\prod = \frac{1}{2}\int_0^L \int_{A_1} (\sigma_{xx}\varepsilon_{xx} - D_x E_x) dA_1 dx \tag{8}$$

Substituting Eqs. (3)–(7) into Eq. (8), electrostatic strain energy for each layer is:

$$\prod_{ij} = \frac{1}{2}\int_o^L \int_{A_{ij}} [\sigma_{xx}\{\frac{\partial U_{ij}}{\partial x} + \frac{1}{2}(\frac{\partial W_{ij}}{\partial x})^2 - z\frac{\partial^2 W_{ij}}{\partial x^2}\} - \{h_{11}\varepsilon_x - \in_{11} \frac{\partial \varphi_{ij}}{\partial x} - h_{11}\alpha_x T\}(\frac{-\partial \varphi_{ij}}{\partial x})]dA_{ij}dx, \quad (9)$$

where i is number of nanotubes and j is the inner or outer layer of nanotubes, where j =1 and 2 represent the outer and inner layer, respectively. The resultant forces and moments in the middle surface of DWBNNT are:

$$\begin{array}{l} N_{xi} = \int_A \sigma_x dA_i \\ M_{xi} = \int_A \sigma_x z dA_i \end{array} \quad (10)$$

Thus, total strain energy leads to:

$$\begin{array}{rcl} \prod\limits_{ij} & = & \frac{1}{2}\int_0^L [N_{xij}\frac{\partial U_{ij}}{\partial x} + \frac{1}{2}N_{xij}(\frac{\partial W_{ij}}{\partial x})^2 - M_{xij}\frac{\partial^2 W_{ij}}{\partial x^2} + h_{11}A_{ij}\frac{\partial U_{ij}}{\partial x}(\frac{\partial \varphi_{ij}}{\partial x}) + \\ & & \frac{1}{2}h_{11}A_{ij}(\frac{\partial W_{ij}}{\partial x})^2(\frac{\partial \varphi_{ij}}{\partial x}) - zh_{11}\frac{\partial^2 W_{ij}}{\partial x^2}\frac{\partial \varphi_{ij}}{\partial x} - 2 \in_{11} A_{ij}(\frac{\partial \varphi_{ij}}{\partial x})^2 - h_{11}\alpha_x T A_{ij}\frac{\partial \varphi_{ij}}{\partial x}]dx \end{array} \quad (11)$$

3.2. External work

For the DWBNNT, interaction forces between the inner and outer tubes are equal in magnitude and opposite in sign and evaluated based on the Lennard-Jones model [16] as:

$$\begin{array}{l} q_{11} = 2\pi r_{11} c(W_{12} - W_{11}) \\ q_{21} = 2\pi r_{21} c(W_{22} - W_{21}) \end{array} \quad (12)$$

where c is vdW interaction coefficient and $W_{ij}(i, j = 1, 2)$ corresponds to the transverse displacement of layers. Therefore, the interaction forces between the inner and outer layer are:

$$\begin{array}{l} q_{11}r_{11} = -q_{12}r_{12} \\ q_{21}r_{11} = -q_{22}r_{12} \end{array} \quad (13)$$

Two DWBNNTs are coupled by a Pasternak foundation, where the spring foundation and shear layer are represented by k_w and G_p terms, respectively. The effect of elastic medium on a coupled system is presented as follows [25]:

$$F_{Elastic\,medium} = \pi r_{12}\left(k_w(w_{12} - w_{22}) - G_p\nabla^2(w_{12} - w_{22})\right) + \pi r_{12}\left(k_w w_{12} - G_p\nabla^2 w_{12}\right) \quad (14)$$

Hence, the external work due to the surrounding elastic medium and vdW interactions can be written as:

$$\Omega_{11} = \frac{1}{2}\int_0^L q_{11}W_{11}dx \quad (15a)$$

$$\Omega_{12} = \frac{1}{2}\int_0^L q_{12}W_{12}dx + \frac{1}{2}\int_0^L -\left(\pi r_{12}\left(k_w(w_{12} - w_{22}) - G_p\nabla^2(w_{12} - w_{22})\right) + \pi r_{12}\left(k_w w_{12} - G_p\nabla^2 w_{12}\right)\right)W_{12}dx \quad (15b)$$

$$\Omega_{21} = \frac{1}{2}\int_0^L q_{21} W_{21} dx \tag{15c}$$

$$\Omega_{22} = \frac{1}{2}\int_0^L q_{22} W_{22} dx + \frac{1}{2}\int_0^L \left(\pi r_{12}\left(k_w(w_{12}-w_{22}) - G_p\nabla^2(w_{12}-w_{22})\right) + \pi r_{12}\left(k_w w_{22} - G_p\nabla^2 w_{22}\right)\right) W_{22} dx \tag{15d}$$

3.3. Hamilton's principle

The higher order governing equations of motion for embedded DWBNNTs can be derived from a dynamic version of the virtual work principle well known as Hamilton's principle:

$$\int_{t_0}^{t_1} (\delta \prod - \delta\Omega)\, dt = 0 \tag{16}$$

Using Eqs. (11) and (15) with Hamilton's principle and integrating Eq. (16) by parts and setting the coefficient of mechanical and electrical to zero, the motion equations are obtained as:

$$\begin{aligned} &\delta U_{ij}: \\ &-\frac{\partial N_{xij}}{\partial x} - h_{11} A_{ij} \frac{\partial^2 \varphi_{ij}}{\partial x^2} = 0 \end{aligned} \tag{17}$$

$$\begin{aligned} &\delta W_{11}: \\ &-\frac{\partial}{\partial x}(N_{x11}\frac{\partial W_{11}}{\partial x}) - \frac{\partial^2 M_{x11}}{\partial x^2} - h_{11}A_{11}(\frac{\partial}{\partial x})(\frac{\partial W_{11}}{\partial x}\frac{\partial \varphi_{11'}}{\partial x}) - q_{11} = 0 \end{aligned} \tag{18}$$

$$\begin{aligned} &\delta W_{12}: \\ &-\frac{\partial}{\partial x}(N_{x12}\frac{\partial W_{12}}{\partial x}) - \frac{\partial^2 M_{x12}}{\partial x^2} - h_{11}A_{12}(\frac{\partial}{\partial x})(\frac{\partial W_{12}}{\partial x}\frac{\partial \varphi_{12'}}{\partial x}) - q_{12} + \\ &h\left(k_w(W_{12}-W_{22}) - G_p\tfrac{\partial^2}{\partial x^2}(W_{12}-W_{22})\right) = 0 \end{aligned} \tag{19}$$

$$\begin{aligned} &\delta W_{21}: \\ &-\frac{\partial}{\partial x}(N_{x21}\frac{\partial W_{21}}{\partial x}) - \frac{\partial^2 M_{x21}}{\partial x^2} - h_{11}A_{21}(\frac{\partial}{\partial x})(\frac{\partial W_{21}}{\partial x}\frac{\partial \varphi_{21}}{\partial x}) - q_{21} = 0 \end{aligned} \tag{20}$$

$$\begin{aligned} &\delta W_{22}: \\ &-\frac{\partial}{\partial x}(N_{x22}\frac{\partial W_{22}}{\partial x}) - \frac{\partial^2 M_{x22}}{\partial x^2} - h_{11}A_{22}(\frac{\partial}{\partial x})(\frac{\partial W_{22}}{\partial x}\frac{\partial \varphi_{22'}}{\partial x}) - q_{22} + \\ &h\left(-k_w(W_{12}-W_{22}) + G_p\frac{\partial^2}{\partial x^2}(W_{12}-W_{22})\right) = 0 \end{aligned} \tag{21}$$

$$\begin{aligned} &\delta \varphi_{ij}: \\ &-h_{ij}A_{ij}\frac{\partial^2 U_{ij}}{\partial x^2} - h_{ij}A_{ij}\frac{\partial^2 W_{ij}}{\partial x^2}\frac{\partial W_{ij}}{\partial x} + 2 \in_{ij} A_{ij}\frac{\partial^2 \varphi_{ij}}{\partial x^2} = 0 \end{aligned} \tag{22}$$

Using Eqs. (1)–(4), Eq. (10) for nonlocal form of force and moment becomes:

$$\begin{aligned} N_x - (e_0a)^2\frac{\partial^2 N_x}{\partial x^2} &= C_{11}A\frac{\partial U_{ij}}{\partial x} + \frac{1}{2}C_{11}A(\frac{\partial W_{ij}}{\partial x})^2 + h_{11}A\frac{\partial \varphi}{\partial x} - C_{11}\alpha_x AT \\ M_x - (e_0a)^2\frac{\partial^2 M_x}{\partial x^2} &= -C_{11}I\frac{\partial^2 W}{\partial x^2} \end{aligned} \tag{23}$$

Dimensionless parameters are defined as follows [24]:

$$\begin{aligned} &\xi = \frac{x}{l} \qquad w_{ij} = \frac{W_{ij}}{r_{ij}} \qquad \eta_{ij} = \frac{l}{r_{ij}} \qquad en = \frac{e_0 a}{l} \\ &\bar{I}_{ij} = \frac{I_{ij}}{A_{ij}r_{ij}^2} \qquad \bar{C}_{ij} = \frac{2\pi r_{12}Cl^2}{EA_{ij}} \qquad \Delta\bar{T} = \alpha_x T \qquad \bar{k}_w = \frac{\pi r_{12}K_w l^2}{EA_{12}} \\ &\bar{G}_p = \frac{\pi r_{12}G_p}{EA_{12}} \qquad \bar{\varphi} = \frac{\varphi h_{11}}{El} \qquad \gamma = \frac{\in_{11} E}{h_{11}^2} \qquad \bar{p}_{ij} = \frac{N_x}{EA_{ij}} \end{aligned} \tag{24}$$

Using Eqs. (24) and substituting Eq. (23) into Eqs. (17)–(22), the dimensionless equations of motion are obtained as follows:

$$\begin{aligned} &\delta U_{ij}: \\ &-\frac{1}{1-v^2}\frac{1}{\eta_{ij}}\frac{\partial^2 u_{ij}}{\partial\xi^2} - \frac{1}{1-v^2}\frac{1}{\eta_{ij}^2}\frac{\partial w_{ij}}{\partial\xi}\frac{\partial^2 w_{ij}}{\partial\xi^2} - \frac{3}{2}\frac{\partial^2\bar{\varphi}_{ij}}{\partial\xi^2} + \frac{1}{2}e_n^2\frac{\partial^4\bar{\varphi}_{ij}}{\partial\xi^4} = 0 \end{aligned} \tag{25}$$

$$\begin{aligned} &\delta W_{11}: \\ &-\frac{1}{1-v^2}\frac{1}{\eta_{11}}\frac{\partial^2 u_{11}}{\partial\xi^2}\frac{\partial w_{11}}{\partial\xi} - \frac{1}{1-v^2}\frac{1}{\eta_{11}}(\frac{\partial w_{11}}{\partial\xi})^2\frac{\partial^2 w_{11}}{\partial\xi^2} - \bar{p}_{11}\frac{\partial^2 w_{11}}{\partial\xi^2} + e_n^2\bar{p}_{11}\frac{\partial^4 w_{11}}{\partial\xi^4} \\ &+\bar{I}_{11}\frac{1}{1-\nu^2}\frac{1}{\eta_{11}^2}\frac{\partial^4 w_{11}}{\partial\xi^4} - \frac{\partial\bar{\varphi}_{11'}}{\partial\xi}\frac{\partial^2 w_{11}}{\partial\xi^2} - 2\frac{\partial^2\bar{\varphi}_{11'}}{\partial\xi^2}\frac{\partial w_{11}}{\partial\xi} \\ &+e_n^2\frac{\partial\bar{\varphi}_{11'}}{\partial\xi}\frac{\partial^4 w_{11}}{\partial\xi^4} + e_n^2\frac{\partial^4\bar{\varphi}_{11'}}{\partial\xi^4}\frac{\partial w_{11}}{\partial\xi} - \bar{c}\frac{\eta_{11}}{\eta_{12}}w_{12} + \bar{c}w_{11} + \bar{c}e_n^2\frac{\eta_{11}}{\eta_{12}}\frac{d^2 w_{12}}{d\xi^2} - \bar{c}e_n^2\frac{d^2 w_{11}}{d\xi^2} = 0 \end{aligned} \tag{26}$$

$$\begin{aligned} &\delta W_{12}: \\ &-\frac{1}{1-v^2}\frac{1}{\eta_{12}}\frac{\partial^2 u_{12}}{\partial\xi^2}\frac{\partial w_{12}}{\partial\xi} - \frac{1}{1-v^2}\frac{1}{\eta_{12}}(\frac{\partial w_{12}}{\partial\xi})^2\frac{\partial^2 w_{12}}{\partial\xi^2} - \frac{A_{11}}{A_{12}}(\bar{p}_{11}\frac{\partial^2 w_{12}}{\partial\xi^2} + \\ &e_n^2\bar{p}_{11}\frac{\partial^4 w_{12}}{\partial\xi^4}) + \bar{I}_{12}\frac{1}{1-\nu^2}\frac{1}{\eta_{12}^2}\frac{\partial^4 w_{12}}{\partial\xi^4} - \frac{\partial\bar{\varphi}_{12}}{\partial\xi}\frac{\partial^2 w_{12}}{\partial\xi^2} - 2\frac{\partial^2\bar{\varphi}_{12}}{\partial\xi^2}\frac{\partial w_{12}}{\partial\xi} + \\ &e_n^2\frac{\partial\bar{\varphi}_{12}}{\partial\xi}\frac{\partial^4 w_{12}}{\partial\xi^4} + e_n^2\frac{\partial^4\bar{\varphi}_{12}}{\partial\xi^4}\frac{\partial w_{12}}{\partial\xi} + \bar{c}\frac{\eta_{12}}{\eta_{11}}w_{12} - \bar{c}\frac{\eta_{12}^2}{\eta_{11}^2}w_{11} - \bar{c}e_n^2\frac{\eta_{12}}{\eta_{11}}\frac{d^2 w_{12}}{d\xi^2} + \\ &\bar{c}e_n^2\frac{\eta_{12}^2}{\eta_{11}^2}\frac{d^2 w_{11}}{d\xi^2} + 2\bar{k}_w w_{12} - \frac{\eta_{12}}{\eta_{22}}\bar{k}_w w_{22} - 2\bar{G}_p\frac{\partial^2 w_{12}}{\partial\xi^2} + \bar{G}_p\frac{\eta_{12}}{\eta_{22}}\frac{\partial^2 w_{22}}{\partial\xi^2} - \\ &2\bar{k}_w e_n^2\frac{\partial^2 w_{12}}{\partial\xi^2} + k_w e_n^2\frac{\eta_{12}}{\eta_{22}}\frac{\partial^2 w_{22}}{\partial\xi^2} + 2\bar{G}_p e_n^2\frac{\partial^4 w_{12}}{\partial\xi^4} - \bar{G}_p e_n^2\frac{\eta_{12}}{\eta_{22}}\frac{\partial^4 w_{22}}{\partial\xi^4} = 0 \end{aligned} \tag{27}$$

$$\begin{aligned}
&\delta W_{21}: \\
&-\frac{1}{1-v^2}\frac{1}{\eta_{21}}\frac{\partial^2 u_{21}}{\partial\xi^2}\frac{\partial w_{21}}{\partial\xi}-\frac{1}{1-v^2}\frac{1}{\eta_{21}}(\frac{\partial w_{21}}{\partial\xi})^2\frac{\partial^2 w_{21}}{\partial\xi^2}-\bar{p}_{21}\frac{\partial^2 w_{21}}{\partial\xi^2} \\
&+e_n^2\bar{p}_{21}\frac{\partial^4 w_{21}}{\partial\xi^4}+\bar{I}_{21}\frac{1}{1-\nu^2}\frac{1}{\eta_{21}^2}\frac{\partial^4 w_{21}}{\partial\xi^4}-\frac{\partial\bar{\varphi}_{21^{\cdot}}}{\partial\xi}\frac{\partial^2 w_{21}}{\partial\xi^2}-2\frac{\partial^2\bar{\varphi}_{21^{\cdot}}}{\partial\xi^2}\frac{\partial w_{21}}{\partial\xi} \\
&+e_n^2\frac{\partial\bar{\varphi}_{21^{\cdot}}}{\partial\xi}\frac{\partial^4 w_{21}}{\partial\xi^4}+e_n^2\frac{\partial^4\bar{\varphi}_{21^{\cdot}}}{\partial\xi^4}\frac{\partial w_{21}}{\partial\xi}-\bar{c}\frac{\eta_{21}}{\eta_{22}}w_{22}+\bar{c}w_{21}+\bar{c}e_n^2\frac{\eta_{21}}{\eta_{22}}\frac{d^2 w_{22}}{d\xi^2}-\bar{c}e_n^2\frac{d^2 w_{21}}{d\xi^2}=0
\end{aligned} \tag{28}$$

$$\begin{aligned}
&\delta W_{22}: \\
&-\frac{1}{1-v^2}\frac{1}{\eta_{22}}\frac{\partial^2 u_{22}}{\partial\xi^2}\frac{\partial w_{22}}{\partial\xi}-\frac{1}{1-v^2}\frac{1}{\eta_{22}}(\frac{\partial w_{22}}{\partial\xi})^2\frac{\partial^2 w_{22}}{\partial\xi^2}-\frac{A_{21}}{A_{22}}(\bar{p}_{21}\frac{\partial^2 w_{22}}{\partial\xi^2}+ \\
&e_n^2\bar{p}_{21}\tfrac{\partial^4 w_{22}}{\partial\xi^4})+\bar{I}_{22}\tfrac{1}{1-\nu^2}\tfrac{1}{\eta_{22}^2}\tfrac{\partial^4 w_{22}}{\partial\xi^4}-\tfrac{\partial\bar{\varphi}_{22}}{\partial\xi}\tfrac{\partial^2 w_{22}}{\partial\xi^2}-2\tfrac{\partial^2\bar{\varphi}_{22}}{\partial\xi^2}\tfrac{\partial w_{22}}{\partial\xi}+ \\
&e_n^2\frac{\partial\bar{\varphi}_{22}}{\partial\xi}\frac{\partial^4 w_{22}}{\partial\xi^4}+e_n^2\frac{\partial^4\bar{\varphi}_{22}}{\partial\xi^4}\frac{\partial w_{22}}{\partial\xi}+\bar{c}\frac{\eta_{22}}{\eta_{21}}w_{22}-\bar{c}\frac{\eta_{22}^2}{\eta_{21}^2}w_{21}-\bar{c}e_n^2\frac{\eta_{22}}{\eta_{21}}\frac{d^2 w_{22}}{d\xi^2}+ \\
&\bar{c}e_n^2\frac{\eta_{22}^2}{\eta_{21}^2}\frac{d^2 w_{21}}{d\xi^2}-\bar{k}_w\frac{\eta_{22}}{\eta_{12}}w_{12}+2\bar{k}_w w_{22}+\bar{G}_p\frac{\eta_{22}}{\eta_{12}}\frac{\partial^2 w_{12}}{\partial\xi^2}-2\bar{G}_p\frac{\partial^2 w_{22}}{\partial\xi^2}+ \\
&\bar{k}_w e_n^2\frac{\eta_{22}}{\eta_{12}}\frac{\partial^2 w_{12}}{\partial\xi^2}-2\bar{k}_w e_n^2\frac{\partial^2 w_{22}}{\partial\xi^2}-\bar{G}_p e_n^2\frac{\eta_{22}}{\eta_{12}}\frac{\partial^4 w_{12}}{\partial\xi^4}+2\bar{G}_p e_n^2\frac{\partial^4 w_{22}}{\partial\xi^4}=0
\end{aligned} \tag{29}$$

$$\begin{aligned}
&\delta\varphi_{ij}: \\
&\frac{\partial^2 u_{ij}}{\partial\xi^2}-e_n^2\frac{\partial^4 u_{ij}}{\partial\xi^4}+\frac{1}{\eta_{ij}}\frac{\partial^2 w_{ij}}{\partial\xi^2}\frac{\partial w_{ij}}{\partial\xi} \\
&-e_n^2\frac{1}{\eta_{ij}}\left\{3\frac{\partial^3 w_{ij}}{\partial\xi^3}\frac{\partial^2 w_{ij}}{\partial\xi^2}+\frac{\partial w_{ij}}{\partial\xi}\frac{\partial^4 w_{ij}}{\partial\xi^4}\right\}-2\eta_{ij}\gamma\frac{\partial^2\bar{\varphi}_{ij}}{\partial\xi^2}+2e_n^2\eta_{ij}\gamma\frac{\partial^4\bar{\varphi}_{ij}}{\partial\xi^4}=0
\end{aligned} \tag{30}$$

4. Solution method

In this section, the DQM is introduced to solve nonlinear higher order equations of motion. In this method the partial derivative of a function with respect to spatial variables at a given discrete point are approximated as a weighted linear sum of the function values at all discrete points chosen in the solution domain. According to this method, the functions u_{ij} , w_{ij} , φ_{ij} , and their derivatives are [26]:

$$\frac{\partial^k}{\partial\xi^k}\left\{u_{ij},w_{ij},\bar{\varphi}_{ij}\right\}|_{\xi=\xi_n}=\sum_{m=1}^{n}C_{nm}^{(k)}(\xi)\{u_{ijm}(\xi_m),w_{ijm}(\xi_m),\bar{\varphi}_{ijm}(\xi_m)\}\qquad i,j=1,2 \tag{31}$$

where the weighting coefficients of first-order derivative Ξ_{ij} are expressed as:

$$\Xi_{ij}^{(1)}=\frac{R(x_i)}{(x_i-x_j)R(x_j)};\qquad i,j=1,2,...,N;\qquad i\neq j \tag{32}$$

The term $R(x_i)$ is defined as:

$$R(x_i)=\prod_{j=1}^{N}(x_i-x_j);\qquad i\neq j \tag{33}$$

and when $i\neq j$

$$\Xi_{ij}^{(1)}=\Xi_{ii}^{(1)}=-\sum_{k=1}^{N}\Xi_{ik}^{(1)};\qquad i=1,2,...,N;\qquad i\neq k;i=j \tag{34}$$

To obtain the weighting coeffcients for the second- to sixth-order derivatives, the matrix multiplication procedure [21] is:

$$\begin{aligned}
\Xi_{ij}^{(2)} &= \sum_{k=1}^{N} \Xi_{ik}^{(1)} \Xi_{kj}^{(1)} \\
\Xi_{ij}^{(3)} &= \sum_{k=1}^{N} \Xi_{ik}^{(1)} \Xi_{kj}^{(2)} = \sum_{k=1}^{N} \Xi_{ik}^{(2)} \Xi_{kj}^{(1)} \\
\Xi_{ij}^{(4)} &= \sum_{k=1}^{N} \Xi_{ik}^{(1)} \Xi_{kj}^{(3)} = \sum_{k=1}^{N} \Xi_{ik}^{(3)} \Xi_{kj}^{(1)} \\
\Xi_{ij}^{(5)} &= \sum_{k=1}^{N} \Xi_{ik}^{(1)} \Xi_{kj}^{(4)} = \sum_{k=1}^{N} \Xi_{ik}^{(4)} \Xi_{kj}^{(1)} \\
\Xi_{ij}^{(6)} &= \sum_{k=1}^{N} \Xi_{ik}^{(1)} \Xi_{kj}^{(5)} = \sum_{k=1}^{N} \Xi_{ik}^{(5)} \Xi_{kj}^{(1)} \quad i,j = 1,2,...,N
\end{aligned} \tag{35}$$

DQM form of mechanical and electrical boundary conditions at both ends in each layer may be written in dimensionless form as:

$$\text{Simple condition:} \quad \begin{aligned} &u_{ij1} = w_{ij1} = 0, \quad \sum_{m=1}^{N} \Xi_{2m}^{(2)} w_{ijm} = 0, \quad at \quad \xi = 0 \\ &u_{ijN} = w_{ijN} = 0, \quad \sum_{m=1}^{N} \Xi_{N-1m}^{(2)} w_{ijm} = 0, \quad at \quad \xi = 1 \end{aligned} \tag{36a}$$

$$\text{Clamp condition:} \quad \begin{aligned} &u_{ij1} = w_{ij1} = 0, \quad \sum_{m=1}^{N} \Xi_{2m}^{(1)} w_{ijm} = 0, \quad at \quad \xi = 0 \\ &u_{ijN} = w_{ijN} = 0, \quad \sum_{m=1}^{N} \Xi_{N-1m}^{(1)} w_{ijm} = 0, \quad at \quad \xi = 1 \end{aligned} \tag{36b}$$

$$\text{Electrical condition:} \quad \begin{aligned} &\varphi_{ij1} = 0, \ at \quad \xi = 0 \\ &\varphi_{ijN} = 0, \ at \quad \xi = 1 \end{aligned} \tag{36c}$$

As DQM solutions are dependent on grid points, the well-accepted cosine interpolation points are chosen for the present analysis. The nonuniform grid points are known as Chebyshev–Gauss–Lobatto points [21,24]:

$$\xi_i = \frac{1}{2}\left[1 - \cos\frac{(i-1)}{(N-1)}\pi\right] \quad i = 1,2,...,N \tag{37}$$

Based on governing equations, the electric potential and axial direction are:

$$\begin{cases} \{u\} = -\left[[k_{21}][k_{11}]^{-1}[k_{12}] - [k_{22}]\right]^{-1}\left[[k_{21}][k_{11}]^{-1}[k_{13}] - [k_{21}]\right]\{w\} \\ \{\varphi\} = -\left[[k_{22}][k_{12}]^{-1}[k_{11}] - [k_{21}]\right]^{-1}\left[[k_{22}][k_{12}]^{-1}[k_{13}] - [k_{23}]\right]\{w\} \end{cases} \tag{38}$$

Using above equations, the governing equations in the transverse direction become:

$$[k]\{w\} = p[D]\{w\} \tag{39}$$

where $[k]$ and $[D]$ are coefficients of modified stiffness matrix and in-plain load, respectively, defined in the appendix. Eq. (38) can be written as:

$$[K]\{w\} = p\{w\}, \tag{40}$$

where

$$[K] = [D]^{-1}[k] \tag{41}$$

5. Numerical results and discussion

The results presented here are based on the following data used for geometry and material properties of a DWBNNT [17,24]:

$$r_{11} = r_{21} = 10.27\,nm \quad r_{12} = r_{22} = 11.43\,nm \quad l/r_{11} = l/r_{21} = 10 \quad h = 0.075\,nm$$
$$\alpha_x = 1.2 \times 10^{-6} \quad \alpha_\theta = 0.6 \times 10^{-6} \quad E = 1.8\,Tpa \quad \nu = 0.34$$
$$h_{11} = 0.95\,C/m \quad c = 9.91 \times 10^{19}\,N/m^3 \quad \rho = 3.4870\,gr/cm^3$$
$$G_p = 2.071273\,N/m$$
$$k_w = 8.9995035 * 10^{17}\,N/m^3$$

The effects of small-scale, spring and shear foundations, electric potential, and different boundary conditions on the nonlinear buckling of coupled DWBNNTs are discussed in detail. Figure 2 illustrates the out-of-phase transverse displacement of coupled DWBNNT layers when the buckling loads are critical. Since the aspect ratio of the outer layer is lower than that of the inner layer, the displacement magnitude of the outer layer is smaller than that of the inner layer of the DWBBNT. In the out-of-phase state, the transverse displacement directions of each DWBNNT are opposite. It is also found that the simply supported boundary conditions are satisfied at both ends of nanotubes where the displacements and moments are zero. Transverse displacements of in-phase state are demonstrated in Figure 3. It can be seen that the mode shape of both DWBNNTs have equal quantity and direction for outer and inner layers, separately. Also similar to Figure 2, the simply supported boundary conditions are satisfied at both ends of nanotubes. Effects of different phases versus dimensionless nonlocal parameter are presented in Figure 4. In the out-of-phase state, the coupled system is more stable than the in-phase state, and so that the magnitude of the buckling load ratio (BLR) is more for the out-of-phase case. Moreover, it is evident that the difference between in-phase and out-of-phase cases increases with increasing nonlocal parameter. The effects of spring and shear modulus of elastic medium on the critical buckling load of coupled DWBNNTs versus dimensionless small-scale parameter for in-phase and out-of-phase states are depicted in Figures 5–7. The buckling load ratio increases by increasing the elastic medium coefficients. The curves in Figure 7 illustrate that the existence of both spring and shearing foundations has a significant effect on the BLR in comparison with spring and shear foundations separately. The BLR versus the aspect ratio (l/r_{11}) for in-phase and out-of-phase cases is shown in Figure 8, where this figure demonstrates the effect of nonlocal parameter on the nonlinear buckling as in previous figures. As can be seen, BLR increases for all values of the nonlocal parameter when the aspect ratio increases, while for the out-of-phase state the BLR is higher than it is for the in-phase case. In fact, in the out-of-phase case the coupled system is stiffer and the BLR is more than it is for the in-phase state. Moreover, by increasing the aspect ratio, the nonlocal results tend to local results. In order to illustrate the impact of boundary conditions on the BLR parameter, 3 different boundary conditions are considered in Figure 9, where the in-phase state has a remarkable effect for all boundary conditions. It is also concluded that for the clamp–clamp boundary condition, the effect of the scale coefficient is greater than

that of the simply supported one in out-of-phase and in-phase. In other words, as boundary conditions become stiffer, BLR will be decreased. Figure 10 depicts the distribution of dimensionless electric potential along the dimensionless DWBNNTs' length for in-phase and out-of-phase states. It can be seen from this figure that dimensionless electric potentials are zero at both ends due to the assumed boundary conditions in Eq. (36c). It is found that the magnitude of dimensionless electric potential for the inner layer is more than that of the outer layer and the in-phase state is greater than the out-of-phase state.

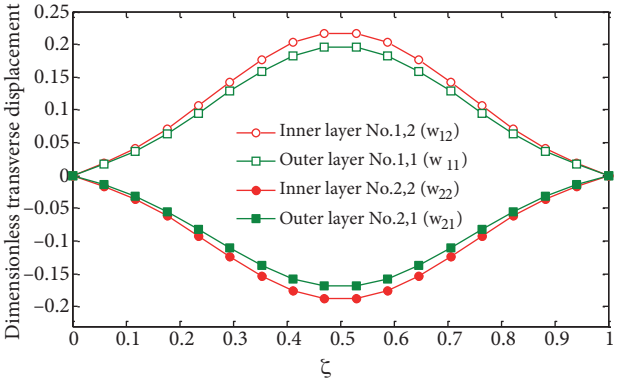

Figure 2. Dimensionless transverse displacement versus $\xi = x/L$ for the out-of-phase state.

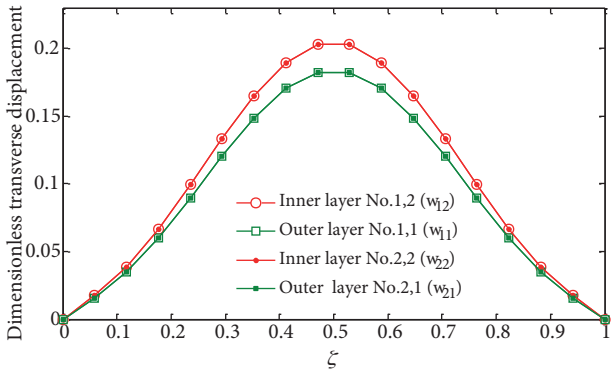

Figure 3. Dimensionless transverse displacement versus $\xi = x/L$ for the in-phase state.

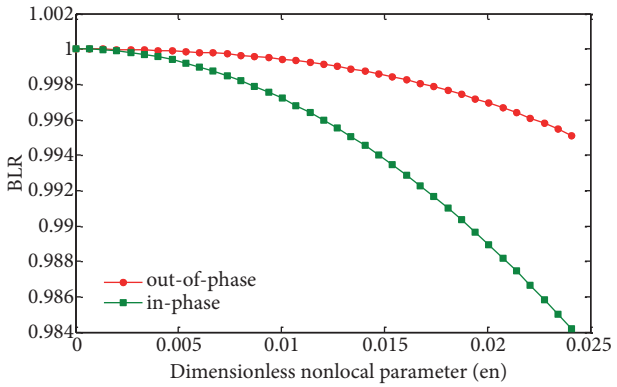

Figure 4. Buckling load ratio versus small-scale parameter for in-phase and out-of-phase states.

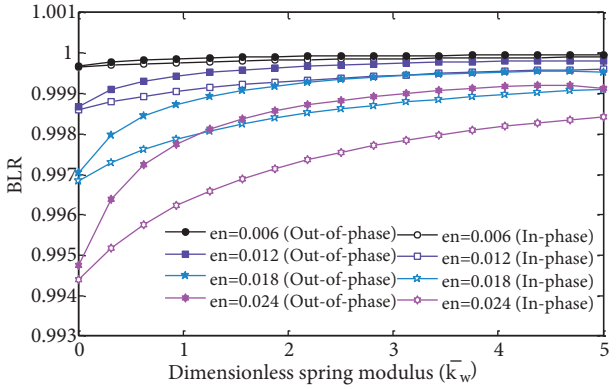

Figure 5. Buckling load ratio versus dimensionless spring modulus.

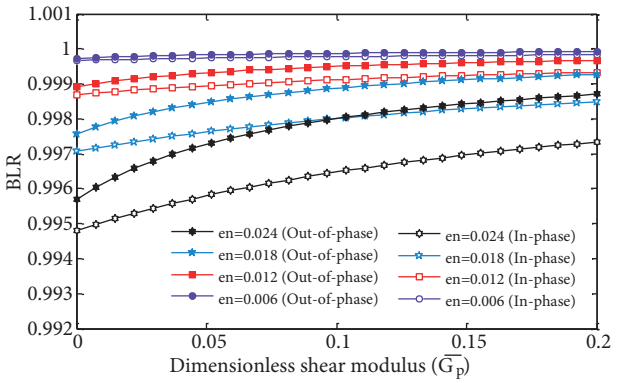

Figure 6. Buckling load ratio versus dimensionless shear modulus.

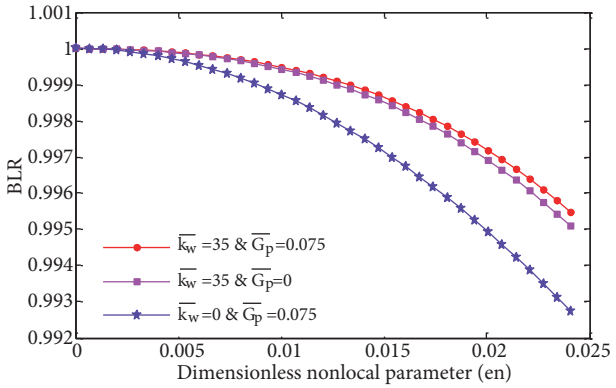

Figure 7. Buckling load ratio versus small-scale parameter for different magnitudes of elastic medium.

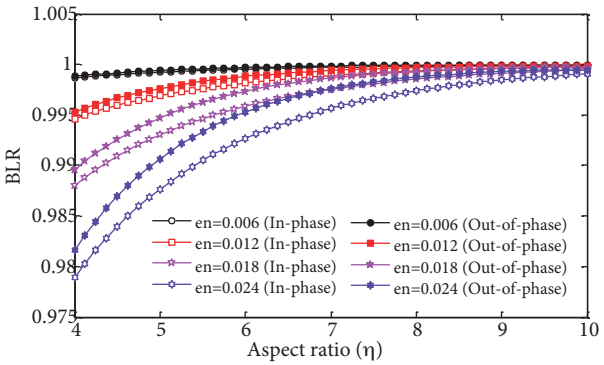

Figure 8. Buckling load ratio versus aspect ratio for different values of dimensionless small-scale parameter.

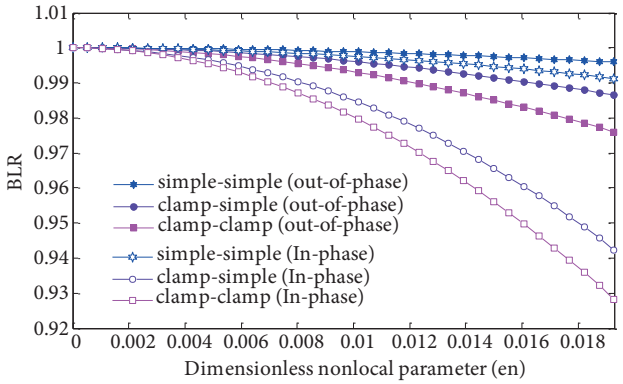

Figure 9. Buckling load ratio versus dimensionless small-scale parameter for different boundary conditions.

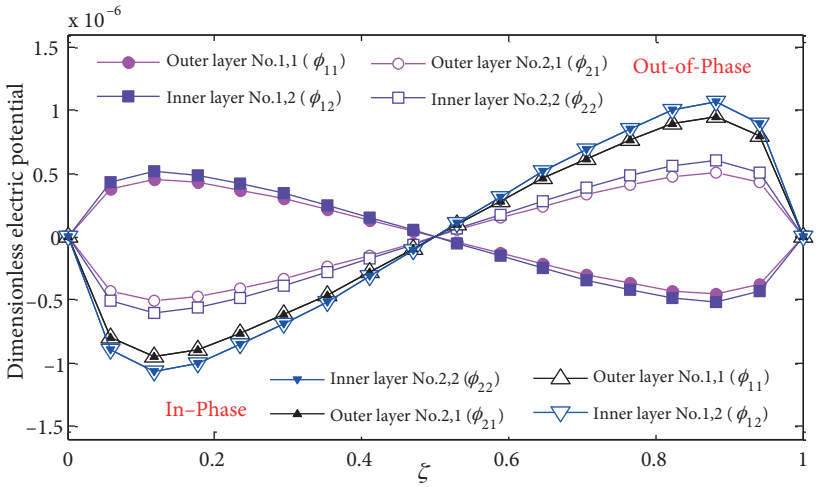

Figure 10. Dimensionless electric potential of each layer along the nanotube length for in-phase and out-of-phase states.

In order to validate the present work, a simplified case of the analysis is studied. For $e_0\,a = 2\ nm$, the buckling load versus aspect ratio of a SWCNT under compression longitudinal load is plotted and compared with previous ones [10,21]. The results obtained by Murmu and Pradhan [21] and Wang et al. [10] are compared with the results of this study in Figure 11. This figure demonstrates that there is very good agreement between them.

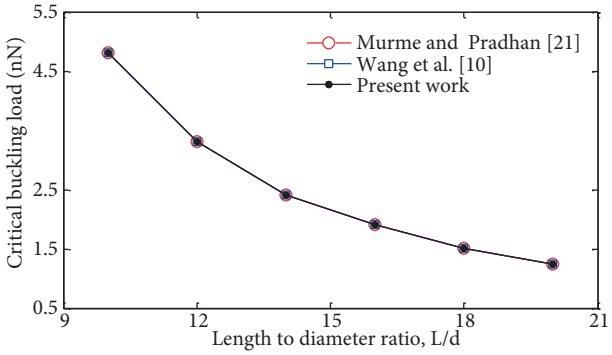

Figure 11. Comparison of the present results with those presented by Murmu and Pradhan (2009) and Wang et al. (2006).

6. Conclusion

Nonlinear buckling response of embedded coupled DWBNNTs subjected to electro-thermo–mechanical loadings was investigated using EBB where 2 DWBNNTs were surrounded by a Pasternak foundation. Nonlinear governing equations were solved numerically with DQM for in-phase and out-of-phase cases. The results indicated that BLR for the in-phase case is greater than it is for the out-of-phase state where in the out-of-phase state the stiffness of the coupled system is more than it is in the in-phase state. Furthermore, the BLR was sensitive to the small-scale coefficient and aspect ratio, so that increasing aspect ratio and decreasing small-scale coefficient lead to increases in BLR. In addition, the effect of clamped boundary condition was more remarkable than the simply supported one for in-phase and out-of-phase states. The results of this study were validated by Murmu and Pradhan [21] and Wang et al. [10]. The findings of present study can be used in advanced applications of nano/micro mechanical devices such as nano/micro-electro–mechanical systems.

Acknowledgments

The author would like to thank the reviewers for their reports to improve the clarity of this article. The authors are grateful to the University of Kashan for supporting this work by Grant no. 65475/38. They would also like to thank the Iranian Nanotechnology Development Committee for their financial support.

Appendix

$$[A] = \begin{bmatrix} k_{11} & k_{12} & k_{13} \\ k_{21} & k_{22} & k_{23} \\ k_{31} & k_{32} & k_{33} \end{bmatrix}$$

$$k_{11} = \begin{bmatrix} a_{11} & [0] & [0] & [0] \\ [0] & a_{12} & [0] & [0] \\ [0] & [0] & a_{21} & [0] \\ [0] & [0] & [0] & a_{22} \end{bmatrix} \quad k_{12} = \begin{bmatrix} b_{11} & [0] & [0] & [0] \\ [0] & b_{12} & [0] & [0] \\ [0] & [0] & b_{21} & [0] \\ [0] & [0] & [0] & b_{22} \end{bmatrix} \quad k_{13} = \begin{bmatrix} c_{11} & [0] & [0] & [0] \\ [0] & c_{12} & [0] & [0] \\ [0] & [0] & c_{21} & [0] \\ [0] & [0] & [0] & c_{22} \end{bmatrix}$$

$$k_{21} = \begin{bmatrix} d_{11} & [0] & [0] & [0] \\ [0] & d_{12} & [0] & [0] \\ [0] & [0] & d_{21} & [0] \\ [0] & [0] & [0] & d_{22} \end{bmatrix} \quad k_{22} = \begin{bmatrix} e_{11} & [0] & [0] & [0] \\ [0] & e_{12} & [0] & [0] \\ [0] & [0] & e_{21} & [0] \\ [0] & [0] & [0] & e_{22} \end{bmatrix} \quad k_{23} = \begin{bmatrix} f_{11} & [0] & [0] & [0] \\ [0] & f_{12} & [0] & [0] \\ [0] & [0] & f_{21} & [0] \\ [0] & [0] & [0] & f_{22} \end{bmatrix}$$

$$k_{31} = \begin{bmatrix} \phi_{11} & [0] & [0] & [0] \\ [0] & \varphi_{12} & [0] & [0] \\ [0] & [0] & \phi_{21} & [0] \\ [0] & [0] & [0] & \phi_{22} \end{bmatrix} \quad k_{32} = \begin{bmatrix} u_{11} & [0] & [0] & [0] \\ [0] & u_{12} & [0] & [0] \\ [0] & [0] & u_{21} & [0] \\ [0] & [0] & [0] & u_{22} \end{bmatrix} \quad k_{33} = \begin{bmatrix} m_{111} & m_{121} & [0] & [0] \\ m_{112} & m_{122} & [0] & m_{222} \\ [0] & [0] & m_{213} & m_{223} \\ [0] & m_{124} & m_{214} & m_{224} \end{bmatrix}$$

$$D = \begin{bmatrix} b_1 & [0] & [0] & [0] \\ [0] & b_2 & [0] & [0] \\ [0] & [0] & d_1 & [0] \\ [0] & [0] & [0] & d_2 \end{bmatrix}$$

$$a_{mn} = -2\eta_{mn}\gamma[C_{ij}^{(2)}] + 2e_n^2\eta_{mn}[C_{ij}^{(4)}]$$

$$b_{mn} = [C_{ij}^{(2)}] - e_n^2[C_{ij}^{(4)}]$$

$$c_{mn} = \left\{ \frac{1}{\eta_{mn}} \sum_{j=1}^{N} C_{ij}^{(1)} w_{mnj} [C_{ij}^{(2)}] - e_n^2 \frac{1}{\eta_{mn}} (3 \sum_{j=1}^{N} C_{ij}^{(3)} w_{mnj} [C_{ij}^{(2)}] + \sum_{j=1}^{N} C_{ij}^{(1)} w_{mnj} [C_{ij}^{(4)}]) \right\}$$

$$d_{mn} = -\frac{3}{2} [C_{ij}^{(2)}] + \frac{1}{2} e_n^2 [C_{ij}^{(4)}]$$

$$e_{mn} = -\frac{1}{1-v^2} \frac{1}{\eta_{mn}} [C_{ij}^{(2)}]$$

$$f_{mn} = -\frac{1}{1-v^2} \frac{1}{\eta_{mn}^2} \sum_{j=1}^{N} C_{ij}^{(1)} w_{mnj} [C_{ij}^{(2)}]$$

$$\phi_{11} = -\sum_{j=1}^{N} C_{ij}^{(2)} w_{11j} [C_{ij}^{(1)}] - 2 \sum_{j=1}^{N} C_{ij}^{(1)} w_{11j} [C_{ij}^{(2)}] + e_n^2 \sum_{j=1}^{N} C_{ij}^{(4)} w_{11j} [C_{ij}^{(1)}] + e_n^2 \sum_{j=1}^{N} C_{ij}^{(1)} w_{11j} [C_{ij}^{(4)}]$$

$$\phi_{12} = -\sum_{j=1}^{N} C_{ij}^{(2)} w_{12j} [C_{ij}^{(1)}] - 2 \sum_{j=1}^{N} C_{ij}^{(1)} w_{12j} [C_{ij}^{(2)}] + e_n^2 \sum_{j=1}^{N} C_{ij}^{(4)} w_{12j} [C_{ij}^{(1)}] + e_n^2 \sum_{j=1}^{N} C_{ij}^{(1)} w_{12j} [C_{ij}^{(4)}]$$

$$\phi_{21} = \sum_{j=1}^{N} C_{ij}^{(2)} w_{21j} [C_{ij}^{(1)}] + 2 \sum_{j=1}^{N} C_{ij}^{(1)} w_{21j} [C_{ij}^{(2)}] - e_n^2 \sum_{j=1}^{N} C_{ij}^{(4)} w_{21j} [C_{ij}^{(1)}] - e_n^2 \sum_{j=1}^{N} C_{ij}^{(1)} w_{21j} [C_{ij}^{(4)}]$$

$$\phi_{22} = \sum_{j=1}^{N} C_{ij}^{(2)} w_{22j} [C_{ij}^{(1)}] + 2 \sum_{j=1}^{N} C_{ij}^{(1)} w_{22j} [C_{ij}^{(2)}] - e_n^2 \sum_{j=1}^{N} C_{ij}^{(4)} w_{22j} [C_{ij}^{(1)}] - e_n^2 \sum_{j=1}^{N} C_{ij}^{(1)} w_{22j} [C_{ij}^{(4)}]$$

$$u_{11} = -\frac{1}{1-\nu^2} \frac{1}{\eta_{11}} \sum_{j=1}^{N} C_{ij}^{(1)} w_{11j} [C_{ij}^{(2)}]$$

$$u_{12} = -\frac{1}{1-\nu^2} \frac{1}{\eta_{12}} \sum_{j=1}^{N} C_{ij}^{(1)} w_{12j} [C_{ij}^{(2)}]$$

$$u_{21} = \frac{1}{1-\nu^2} \frac{1}{\eta_{21}} \sum_{j=1}^{N} C_{ij}^{(1)} w_{21j} [C_{ij}^{(2)}]$$

$$u_{22} = \frac{1}{1-\nu^2} \frac{1}{\eta_{22}} \sum_{j=1}^{N} C_{ij}^{(1)} w_{22j} [C_{ij}^{(2)}]$$

$$m_{111} = -\frac{1}{1-v^2} \frac{1}{\eta_{11}^2} (\sum_{j=1}^{N} C_{ij}^{(1)} w_{11j})^2 [C_{ij}^{(2)}] + \bar{c}_{11} I - \bar{c}_{11} e_n^2 [C_{ij}^{(2)}] + \bar{I}_{11} \frac{1}{1-\nu^2} \frac{1}{\eta_{11}^2} [C_{ij}^{(4)}]$$

$$m_{121} = -\bar{c}_{11} \frac{\eta_{11}}{\eta_{12}} I + \bar{c}_{11} e_n^2 \frac{\eta_{11}}{\eta_{12}} [C_{ij}^{(2)}]$$

$$m_{112} = -\bar{c}_{12} \frac{\eta_{12}^2}{\eta_{11}^2} I + \bar{c}_{12} e_n^2 \frac{\eta_{12}^2}{\eta_{11}^2} [C_{ij}^{(2)}]$$

$$m_{122} = -\frac{1}{1-\nu^2}\frac{1}{\eta_{12}^2}(\sum_{j=1}^{N} C_{ij}^{(1)} w_{12j})^2[C_{ij}^{(2)}] + \bar{I}_{12}\frac{1}{1-\nu^2}\frac{1}{\eta_{12}^2}[C_{ij}^{(4)}] + \bar{c}_{12}\frac{\eta_{12}}{\eta_{11}}I - \bar{c}_{12}(e_n^2)\frac{\eta_{12}}{\eta_{11}}[C_{ij}^{(2)}] + 2(k_w I - G_p[C_{ij}^{(2)}] - k_w(e_n^2)[C_{ij}^{(2)}] + G_p(e_n^2)[C_{ij}^{(4)}])$$

$$m_{222} = k_w\frac{\eta_{12}}{\eta_{22}}I - G_p\frac{\eta_{12}}{\eta_{22}}[C_{ij}^{(2)}] - k_w e_n^2\frac{\eta_{12}}{\eta_{22}}[C_{ij}^{(2)}] + G_p e_n^2\frac{\eta_{12}}{\eta_{22}}[C_{ij}^{(4)}]$$

$$m_{213} = -(-\frac{1}{1-\nu^2}\frac{1}{\eta_{21}^2}(\sum_{j=1}^{N} C_{ij}^{(1)} w_{21j})^2[C_{ij}^{(2)}] + \bar{c}_{21}I - \bar{c}_{21}e_n^2[C_{ij}^{(2)}] + \bar{I}_{21}\frac{1}{1-\nu^2}\frac{1}{\eta_{21}^2}[C_{ij}^{(4)}])$$

$$m_{223} = -(-\bar{c}_{21}\frac{\eta_{21}}{\eta_{22}}I + \bar{c}_{21}e_n^2\frac{\eta_{21}}{\eta_{22}}[C_{ij}^2])$$

$$m_{124} = -(k_w\frac{\eta_{22}}{\eta_{12}}I - G_p\frac{\eta_{22}}{\eta_{12}}[C_{ij}^{(2)}] - k_w e_n^2\frac{\eta_{22}}{\eta_{12}}[C_{ij}^{(2)}] + G_p e_n^2\frac{\eta_{22}}{\eta_{12}}[C_{ij}^{(4)}])$$

$$m_{214} = -(-\bar{c}_{22}\frac{\eta_{22}^2}{\eta_{21}^2}I + \bar{c}_{22}e_n^2\frac{\eta_{22}^2}{\eta_{21}^2}[C_{ij}^{(2)}])$$

$$m_{224} = -(-\tfrac{1}{1-\nu^2}\tfrac{1}{\eta_{22}^2}(\sum_{j=1}^{N} C_{ij}^{(1)} w_{22j})^2[C_{ij}^{(2)}] + \bar{I}_{22}\tfrac{1}{1-\nu^2}\tfrac{1}{\eta_{22}^2}[C_{ij}^{(4)}] + \bar{c}_{22}\tfrac{\eta_{22}}{\eta_{21}}I - \bar{c}_{22}e_n^2\tfrac{\eta_{22}}{\eta_{21}}[C_{ij}^{(2)}]) + 2(-k_w I + G_p[C_{ij}^{(2)}] + k_w e_n^2[C_{ij}^{(2)}] - G_p e_n^2[C_{ij}^{(4)}])$$

$$b_1 = C_{ij}^{(2)} - e_n^2[C_{ij}^{(4)}]$$

$$b_2 = \frac{a_{11}}{a_{22}}([C_{ij}^{(2)}] - e_n^2[C_{ij}^{(4)}])$$

$$d_1 = -([C_{ij}^{(2)}] - e_n^2[C_{ij}^{(4)}])$$

$$d_2 = -\frac{a_{11}}{a_{22}}([C_{ij}^{(2)}] - e_n^2[C_{ij}^{(4)}])$$

$$[k] = [-[k_{32}][[k_{21}][k_{11}]^{-1}[k_{12}] - [k_{22}]]^{-1}[[k_{21}][k_{11}]^{-1}[k_{13}] - [k_{21}]] + [k_{33}] - k_{31}[[k_{22}][k_{12}]^{-1}[k_{11}] - [k_{21}]]^{-1}[[k_{22}][k_{12}]^{-1}[k_{13}] - [k_{23}]]]$$

References

[1] Iijima S. Helical microtubules of graphitic carbon. Nature 1991; 354: 56–58.

[2] Rubio A, Corkill JL, Cohen ML. Theory of graphitic boron nitride nanotubes. Phys Rev B 1994; 49: 5081–5084.

[3] Laude T, Matsui Y, Marraud A, Jouffrey B. Long ropes of boron nitride nanotubes grown by a continuous laser heating. Appl Phys Lett 2000; 76: 3239–3241.

[4] Zhang S, Yu F, Piezoelectric materials for high temperature sensors. J Am Ceram Soc 2011; 94: 3153–3170.

[5] Wildoer JWG, Venema LC, Rinzler AG, Smalley RE, Dekker C. Electronic structure of atomically resolved carbon nanotubes. Nature 1998; 391: 59–62.

[6] Arya SPS, Amico AD. Preparation, properties and applications of boron nitride thin films. Thin Solid Films 1988; 157: 267–282.

[7] Golberg D, Bando YC, Tang C, Zhi CY. Boron nitride nanotubes. Adv Mater 2007; 19: 2413–2432.

[8] Eringen AC. On differential equations of nonlocal elasticity and solutions of screw dislocation and surface waves. J Appl Phys 1983; 54: 4703–4710.

[9] Wang Q, Varadan VK. Vibration of carbon nanotubes studied using nonlocal continuum mechanics. Smart Mater Struct 2006; 15: 659–666.

[10] Wang CM, Zhang YY, Ramesh SS, Kitipornchai S. Buckling analysis of micro- and nano-rods/tubes based on nonlocal Timoshenko beam theory. J Phys D Appl Phys 2006; 39: 3904–3909.

[11] Reddy JN. Nonlocal theories for bending, buckling and vibration of beams. Int J Eng Sci 2007; 45: 288–307.

[12] Aydogdu M. A general nonlocal beam theory: Its application to nanobeam bending, buckling and vibration. Physica E 2009; 41: 1651–1655.

[13] Ghorbanpour Arani A, Mohammadimehr M, Arefmanesh A, Ghasemi A. Transverse vibration of short carbon nanotube using cylindrical shell and beam models. Proc Inst Mech Eng Part C 2010; 24: 745–56.

[14] Ghorbanpour Arani A, Zarei MS, Mohammadimehr M, Arefmanesh A, Mozdianfard MR. The thermal effect on buckling analysis of a DWCNT embedded on the Pasternak foundation. Physica E 2011; 43: 1642–1648.

[15] Akgöz B, Civalek Ö. Strain gradient elasticity and modified couple stress models for buckling analysis of axially loaded micro-scaled beams. Int J Eng Sci 2011; 49: 1268–1280.

[16] Salehi-Khojin A, Jalili N. Buckling of boron nitride nanotube reinforced piezoelectric polymeric composites subject to combined electro–thermo-mechanical loadings. Compos Sci Technol 2008; 68: 1489–1501.

[17] Ghorbanpour Arani A, Amir S, Shajari AR, Mozdianfard MR. Electro–thermo-mechanical buckling of DWBNNTs embedded in bundle of CNTs using nonlocal piezoelasticity cylindrical shell theory. Composites Part B 2012; 43: 195–203.

[18] Murmu T, Adhikari S. Nonlocal vibration of bonded double-nanoplate-systems. Composites Part B 2011; 42: 1901–1911.

[19] Murmu T, Sienz J, Adhikari J, Arnold C, Nonlocal buckling behavior of bonded double-nanoplate-systems. J Appl Phys 2011; 110: 084316.

[20] Ghorbanpour Arani A, Shiravand A, Rahi M, Kolahchi R. Nonlocal vibration of coupled DLGS systems embedded on Visco-Pasternak foundation. Physica B 2012; 407: 4123–4131.

[21] Murmu T, Pradhan SC. Buckling analysis of a single-walled carbon nanotube embedded in an elastic medium based on nonlocal elasticity and Timoshenko beam theory and using DQM, Physica E 2009; 41: 1232–1239.

[22] Ghorbanpour Arani A, Shajari AR, Amir S, Loghman A. Electro-thermo-mechanical nonlinear nonlocal vibration and instability of embedded micro-tube reinforced by BNNT conveying fluid. Physica E 2012; 45: 109–121.

[23] Ghorbanpour Arani A, Amir S, Shajari AR, Mozdianfard MR, Khoddami Maraghi Z, Mohammadimehr M. Electro-thermal non-local vibration analysis of embedded DWBNNTs. Proc Inst Mech Eng Part C 2011; 224: 745–756.

[24] Khoddami Maraghi Z, Ghorbanpour Arani A, Kolahchi R, Amir S, Bagheri MR. Nonlocal vibration and instability of embedded DWBNNT conveying viscose fluid. Composites Part B 2013; 45: 423–432.

[25] Paliwal DN, Pendey RK, Nath T. Free vibrations of circular cylindrical shell on Winkler and Pasternak foundations. Int J Press Vessels Pip 1996; 69: 79–89.

[26] Ke LL, Wang YSh. Flow-induced vibration and instability of embedded double-walled carbon nanotubes based on a modified couple stress theory. Physica E 2011; 43: 1031–1039.